The origin and maintenance of metabolic allometry in animals

Craig R. White[1,2,*], Dustin J. Marshall[2], Lesley A. Alton[1,2], Pieter A. Arnold[1,3], Julian E. Beaman[1], Candice L. Bywater[2,4], Catriona Condon[5], Taryn S. Crispin[1], Aidan Janetzki[1], Elia Pirtle[4], Hugh S. Winwood-Smith[1], Michael J. Angilletta Jr.[5], Stephen F. Chenoweth[1], Craig E. Franklin[1], Lewis G. Halsey[6], Michael R. Kearney[4], Steven J. Portugal[7], Daniel Ortiz-Barrientos[1]

[1]School of Biological Sciences, The University of Queensland, Queensland, Australia 4072

[2]Centre for Geometric Biology, School of Biological Sciences, Monash University, Victoria, Australia, 3800.

[3]Research School of Biology, The Australian National University, Acton, Australian Capital Territory, Australia 2601

[4]School of Biosciences, The University of Melbourne, Parkville Campus, Victoria, Australia, 3010

[5]School of Life Sciences, Arizona State University, Tempe, Arizona 85287, USA

[6]Department of Life Sciences, University of Roehampton, Holybourne Avenue, London SW15 4JD, UK

[7]School of Biological Sciences, Royal Holloway, University of London, Egham, Surrey, TW20 0EX, UK

*e-mail: craig.white@monash.edu

Organisms vary widely in size from microbes weighing 0.1 picograms to trees weighing thousands of megagrams, a 10^{21}-fold range similar to the difference in mass between an elephant and the Earth. Mass has a pervasive influence on biological processes but the effect is usually non-proportional; for example, a 10-fold increase in mass is typically accompanied by just a 4-to-7-fold increase in metabolic rate. Understanding the cause of allometric scaling has been a long-standing problem in biology. Here, we examine the evolution of metabolic allometry in animals by linking microevolutionary processes to macroevolutionary patterns. We show that the genetic correlation between mass and metabolic rate is strong and positive in insects, birds, and mammals. We then use these data to simulate the macroevolution of mass and metabolic rate, and show that the interspecific relationship between these traits in animals is consistent with evolution under persistent multivariate selection on mass and metabolic rate over long periods of time.

Animals expend energy to survive, forage, grow, and reproduce, and the processes that cause variation in metabolic rate have fascinated biologists for over a century[1-11]. Metabolic rates integrate many organismal functions[12], and relate to several traits that enhance fitness (e.g., social dominance, offspring growth, and lifetime reproductive success[8,13-15]). Because energy turnover varies according to size, measurements of metabolic rate (*MR*) and body mass (*M*) are usually strongly correlated. Among species of birds and mammals, for example, more than 94% of the variance in *MR* can be explained by *M* alone[16-18]. Surprisingly, however, *MR* is not linearly proportional to *M*; instead, *MR* is proportional to M^b, where *b* is typically less than one [6,9], especially for resting *MR* and daily mean *MR* of free-living animals[19]; *b* is often higher and can approach isometry (*b*=1) for maximally-active animals[7]. Mechanistic hypotheses proposed to explain the observed relationships between *MR* and *M* have invoked variation in a range of physical constraints such as the geometry of circulatory networks[4,5], the need to dissipate heat[7,20], or surface area-volume ratios that influence the flux of nutrients or wastes[21-23]. Other approaches that explain variation in metabolic scaling have invoked biotic and abiotic drivers such as lifestyle and temperature[24], foraging[25], predation[26], and a range of others[7-9,27,28], or differences in body size optimization and the distributions of intraspecific production and mortality parameters across species[29]. Here we complement these studies by investigating microevolutionary and macroevolutionary processes responsible for variation in scaling of metabolic rate in animals.

Theory predicts that microevolutionary processes can lead to macroevolutionary associations between *MR* and *M* in at least two ways:

1. Metabolic allometry could arise due to constraints in the genetic architecture of traits, with little to no role for selection coupled with random evolution[30]. When two traits share genetic variance, through pleiotropy, they do not evolve independently[31] thus the evolution of *MR* and *M* could be constrained if the two traits are genetically correlated. Under this scenario, a macroevolutionary relationship between *MR* and *M* is expected to arise and persist even in the absence of selection.

2. Metabolic allometry could also arise through correlational selection increasing the covariance between *MR* and *M* [30,32]. Under this model, natural selection favours particular combinations of *MR* and *M* over others, and it is the pattern of multivariate selection that gives rise to the sub-linear scaling of *MR* with *M*. This model implies that fitness would differ between individuals with the same mass-specific *MR* (= MR/M) and different *M*; fitness would be highest for small individuals with high mass-specific *MR* and for large individuals with low mass-specific *MR*.

To distinguish between these two explanations (hereafter random evolution, and correlational selection), we took a three-pronged approach: first, we estimated the distribution and strength of the genetic correlation between *MR* and *M* for a suite of species across 800 million years of animal evolution. Using the distribution of genetic correlations between *MR* and *M* and the distributions of the genetic variances of these traits, we next simulated repeatedly the evolution of *MR* and *M* along a phylogeny. This process generated a distribution of values for each of these traits, from which we could calculate the variation in both the scaling exponent of *MR* and the magnitude of residual variation in *MR* (the variation in *MR* that is not explained by variation in *M*). We then compared the distributions of the simulated data with empirical data. If the distribution of simulated values of the scaling exponent *b* and the distribution of simulated residual (mass-independent) variation in *MR* both match their empirical distributions, the allometric scaling of *MR* with *M* could have resulted from random evolution. If, on the other hand, the distribution of simulated values of *b* does not match the empirical distribution, or if the simulated residual variation of *MR* is greater than that of the empirical data, this would demonstrate that the allometric scaling of *MR* with *M* is instead consistent with evolution under correlational selection.

Results

As was the case in previous studies of birds[33-35] and mammals[36], our own empirical estimates for three species of insects revealed that the genetic correlation (r_G) between *M* and resting *MR* is positive and strong (Fig. 1). In a previous study of speckled cockroaches *Nauphoeta cinerea*[37], we determined the additive genetic correlation using a paternal half sibling-full sibling breeding design (n = 637 individuals; 48 half-sibling families, 126 full-sibling families). In a previous study of fruit flies *Drosophila melanogaster* (n = 247 individuals), we measured the metabolic rates and dry body masses of 85 isofemale lines[38]. In the present study, we measured metabolic rates and body masses of 438 individual *Drosophila serrata* from 45 isofemale lines created from natural populations. For both species of *Drosophila*, we determined genetic correlations among isofemale lines (see Supplementary Information for details). For all three species of insect, a strong positive genetic correlation was observed (*Nauphoeta cinerea* males: 0.98 ± 0.18 [SE], females: 0.50 ± 0.37; *Drosophila melanogaster*: 0.48 ± 0.17; *Drosophila serrata*: 0.99 ± 0.17). For the full data set including birds and mammals, r_G values range from 0.40 ± 0.35 to 1.18 ± 0.46 (Fig. 1).

To evaluate theoretical predictions, we first explored whether random evolution could have produced the observed distribution of interspecific scaling exponents (*b*). We simulated

the evolution of *MR* and *M* along phylogenies (e.g. Fig. 2), and compared our simulated data with an empirical distribution of *b* estimated from 4,794 means of *MR* and *M* for 2,168 species. These data include 3,799 of our own measurements of *MR* for 2,936 individuals of 32 species in addition to those compiled from the literature (all data are provided in the Supplementary Material).

The empirical estimates of *b* for resting, free-living, and active animals (Supplementary Figure 1) fall within the simulated distribution based on the genetic correlation between *MR* and *M* and their genetic variances (Figs 3a,b). The empirical values for the residual variances also fall within the simulated distribution (Fig. 3c,d). The tails of the simulated distributions are long (Fig. 3), however, and the 95% density contour of the simulated data includes regions of parameter space far outside of the narrow region occupied by the empirical data (Fig. 4). The relationship between *MR* and *M* is therefore far more constrained than expected by chance, and we conclude that the macroevolutionary relationship between *MR* and *M* arises as a consequence of correlational selection on these traits. This conclusion is robust to the underlying distribution of the ratio of σ^2_{MR} *to* σ^2_M used in the simulations (Supplementary Figures 2-4)

Discussion

Theory predicts that responses to selection on a trait initially depend on the genetic correlations between traits, but they are determined by a balance between the intensities of stabilizing and directional selection over longer time scales[32]. Genetic correlations can arise by chance[39] and as a consequence of multivariate selection[40-42]. We hypothesise that the apparent persistence of the genetic correlation between *MR* and *M* over at least some narrow regions of the tree of life suggests that multivariate selection is likely responsible for the distribution of genetic correlations observed in extant species (Fig. 1). Such multivariate selection acting on *MR* and *M* could also act to constrain the observed distributions of these traits, restricting the empirical distributions of *b* and residual variances to the narrow range observed relative to simulations (Fig. 4). Genetic correlations can vary among environments[43], as can intraspecific metabolic scaling relationships[24,26,27,44], and so comparisons of the genetic (co)variances of *MR* and *M* for animals reared or evolved in multiple environments would also be valuable and might provide insight into how the strength and direction of multivariate selection varies among environments. Such data may be particularly useful in explaining the shifts in metabolic scaling that are observed across the tree of life[11].

Multivariate selection on *MR* and *M* could result from physical constraints associated with nutrient mobilisation[23,45,46], nutrient transport[4,5], heat dissipation[7,20], the exchange of nutrients or wastes across surfaces[21,22], or combinations of these acting on different combinations of *MR* and *M*. Variation in the relative contribution of these physical constraints, or their mediation by environmental context, might also contribute to variation in the scaling exponent of metabolic rate[8,23,45,46]. Yet despite the considerable interest in these mechanistic hypotheses, variation in these functional characteristics of organisms have not been empirically linked to measurements of fitness, either directly or indirectly via variation in *MR*; indeed, measurements of the link between lifetime reproductive success and *MR* are exceedingly rare[10]. Future work could fill this knowledge gap by examining how the putative mechanistic drivers of metabolic scaling determine the functional basis of variation in fitness.

Our results show that interspecific relationship between metabolic rate and body mass in animals is consistent with evolution under persistent multivariate selection. The strong positive genetic correlation between *MR* and *M* is present in species of insect, bird, and mammal spanning around 800 million years of evolution (Fig. 1) and might have arisen as a consequence of persistent multivariate selection. These factors – random evolution, multivariate selection, and a persistent genetic correlation – link the micro- and macro-evolution of *MR* and *M* thereby explaining the multivariate distributions of these fundamental traits across the animal tree of life (Fig. 5): microevolutionary processes dictate the trait space available to organisms, and macroevolutionary patterns describe the regions of trait space that are selected over long periods of time.

Methods

Measurements of metabolic rates

Metabolic rates were measured using standard positive pressure flow-through respirometry[47], using techniques that are described in detail elsewhere (e.g. [37,38]) and in the supplementary material. Briefly, air was scrubbed of CO_2 and water vapour before being passed at a known flow rate through a chamber containing an animal, and the concentration of CO_2, or the concentrations of O_2 and CO_2, were measured in the excurrent air. Rates of CO_2 production and O_2 consumption were then calculated using standard equations[47]. For systems in which only CO_2 was measured, rates of CO_2 production were converted to rates of O_2 consumption assuming a respiratory exchange ratio (RER) of 0.8 (RER = rate of CO_2 production divided by rate of O_2 production).

Determination of genetic correlations

For *Drosophila serrata*, genetic (among-line) correlations between body mass and metabolic rate, conditioned on activity and age (ref [48]), were calculated using ASReml-R v3.0 (ref [49]) in R v2.0.2. Approximate standard errors for the estimate of the genetic correlation were calculated using the R 'pin' function[50]. For *Drosophila melanogaster*, genetic (among-line) correlations between dry body mass and metabolic rate, conditioned on temporal block, population, and measurement temperature (ref [48]), were calculated.

Simulations of trait evolution

We simulated the evolution of $\log_{10}M$ and $\log_{10}MR$ over randomly generated phylogenies with 4,000 tips using the 'pbtree' function of the phytools[51] package in R[52]. Preliminary analyses showed that the results were qualitatively similar when larger trees were used, but processing time was considerably increased; we therefore selected a value of 4,000 tips because it is similar to the number of extant species of mammal. Results were also similar if a real tree with branch lengths in units of time was used[53]. We simulated trait values using the 'sim.corrs' function of phytools to conduct Brownian motion simulation on a tree with evolutionary correlations between characters[51]. We set the starting values for the simulation as the medians of $\log_{10}$-transformed M and basal MR for mammals[54]; the simulated distributions of b and mass-independent MR are unaffected by these starting values, which influence only the means of $\log_{10}M$ and $\log_{10}MR$ for the simulated data, not their (co)variances. We set the variance for $\log_{10}M$ (σ^2_M) at 0.025 to yield simulated body masses for extant taxa at the tip of the tree that span a biologically realistic range. We calculated the variance for $\log_{10}MR$ (σ^2_{MR}) based on a distribution of 100,000 values generated using a Weibull distribution (shape = 3.23, scale = 0.818) fitted to the empirical distribution of four values of the ratio of σ^2_{MR} to σ^2_M calculated using log-log transformed data for *Drosophila serrata* (0.81), *Drosophila melanogaster* (0.55), and male and female *Nauphoeta cinerea* (1.1 and 0.47, respectively). We set covariances at $r_G\sqrt{\sigma^2_{MR}}\sqrt{\sigma^2_M}$, where we generated a distribution of 100,000 values of r_G based on the distribution of Fisher's Z-transformed values of r_G for extant species (mean Z = 1.55, s.d. = 1.18, n = 9; for Z-transformation, estimates of $r_G \geq 1$ were substituted with values of 0.999; there was no systematic difference between estimates of Z calculated using log-transformed or untransformed data [t_7 = 0.156, p = 0.86], and so all data were pooled). In each simulation, traits evolved randomly by Brownian motion along the tree (e.g., Fig. 2), and we replicated the simulation 100,000 times.

Compilation of comparative data for body mass and metabolic rate

To test the predictions of our simulations, we assembled a database of body mass and metabolic rate data, which includes measurements of resting animals (basal metabolic rate[55] for birds and mammals, standard metabolic rate[55] for insects, fish, amphibians, and reptiles), free-living animals (daily energy expenditure[56] for reptiles, birds, and mammals) and animals exercising at or near their aerobic limits in a laboratory setting (maximum aerobic metabolic rate[57] for terrestrial mammals and cursorial birds, maximum rate of oxygen uptake for fish[58], and *MR* during flight for insects, bats, and birds). In addition to our measurements of metabolic rate (Supplementary Table 1), we assembled published databases and generated new compilations where published databases were not available (Supplementary Table 2).

For our new compilations of insect standard metabolic rate (Supplementary Table 3) and flight metabolic rate (Supplementary Table 4), reptile field metabolic rate (Supplementary Table 5), and bird field metabolic rate (Supplementary Table 6) and maximum metabolic rate (Supplementary Table 7), we searched online databases (Google Scholar and Web of Science) using key words that identified the measurements of interest ("metabolic rate" or "rate of oxygen consumption" or "rate of carbon dioxide production" or respirometry or calorimetry or "doubly labelled water" or "daily energy expenditure" or "aerobic capacity"). For each of the records identified by this search, we first scanned the title to determine if a record was likely to contain data or citations to data. If the title was promising, we reviewed the abstract, and if that was promising we reviewed the full text. For each record that was reviewed at the full text level, we also searched for cited papers that might contain data. We did not, unfortunately, maintain a tally of how many records were retrieved or how many papers were reviewed at each level. The full database of metabolic rates includes species that vary in size from ants to elephants (0.1 miligrams - 2.6 megagrams). Metabolic rates ranged from 35 picolitres of O_2 per minute for resting weevils (0.5 mg) to 3.6 litres of O_2 per minute for exercising horses (450 kg).

Determination of empirical scaling exponents

We calculated the scaling exponent of metabolic rate, *b*, for each taxonomic group (insects, fish, amphibians, reptiles, birds, and mammals) and each metabolic state (resting, free-living, and exercising) using phylogenetic mixed models[59-61] with phylogenetic relationships from v3 of the open tree of life[62]. We implemented phylogenetic mixed models using ASReml-R v3.0 (ref [49]) and R v3.0.2, with inverse relatedness matrices calculated from phylogenetic covariance matrices using the MCMCglmm package v2.21 [63]. Models for endotherms and free-living reptiles included $\log_{10}MR$ as a response and $\log_{10}M$ as a predictor,

and all other models for ectotherms included $\log_{10}MR$ as a response and both $\log_{10}M$ and measurement temperature as predictors. The parameter estimate for $\log_{10}M$ in each of these models represents the scaling exponent of *MR* (see ref [9]).

Data Availability Statement

All data generated or analysed during this study are included in this published article (and its supplementary information files).

Acknowledgements

This research was supported by the Australian Research Council (projects DP110101776, FT130101493, DP170101114, DP180103925).

Author Contributions

C.R.W., D.O.-B., and D.J.M. designed the study. C.R.W., L.A.A., P.A.A., J.E.B., C.L.B., C.C., T.S.C., A.J., E.P., H.S.W.-S., M.J.A., S.F.C., C.E.F., L.G.H., M.R.K., and S.J.P. collected data. C.R.W. analysed data. C.R.W. and D.O.B. wrote the first version of the manuscript, and all authors contributed to and approved the final version.

Declaration of Competing Interests

The authors declare no competing interests.

References

1 Vernon, H. M. The physiological evolution of the warm-blooded animal. *Sci. Prog.* **7**, 378 (1898).

2 Krogh, A. *Respiratory exchange of animals and man*. (Longmans, Green and Co., 1916).

3 Schmidt-Nielsen, K. *Scaling: Why is animal size so important?* , (Cambridge University Press, 1984).

4 West, G. B., Brown, J. H. & Enquist, B. J. A general model for the origin of allometric scaling laws in biology. *Science* **276**, 122-126 (1997).

5 West, G. B., Brown, J. H. & Enquist, B. J. The fourth dimension of life: Fractal geometry and allometric scaling of organisms. *Science* **284**, 1677-1679 (1999).

6 Glazier, D. S. Beyond the '3/4-power law': variation in the intra- and interspecific scaling of metabolic rate in animals. *Biological Reviews* **80**, 1-52 (2005).

7 Glazier, D. S. A unifying explanation for diverse metabolic scaling in animals and plants. *Biological Reviews* **85**, 111-138 (2010).

8 White, C. R. & Kearney, M. R. Determinants of inter-specific variation in basal metabolic rate. *J. Comp. Physiol. B* **183**, 1-26 (2013).

9 White, C. R. & Kearney, M. R. Metabolic scaling in animals: methods, empirical results, and theoretical explanations. *Comprehensive Physiology* **4**, 231-256 (2014).

10 Pettersen, A. K., Marshall, D. J. & White, C. R. Understanding variation in metabolic rate. *J. Exp. Biol.* **221**, jeb166876 (2018).

11 Uyeda, J. C., Pennell, M. W., Miller, E. T., Maia, R. & McClain, C. R. The evolution of energetic scaling across the vertebrate tree of life. *Am. Nat.* **190**, 185-199, doi:10.1086/692326 (2017).
12 Brown, J. H., Gillooly, J. F., Allen, A. P., Savage, V. M. & West, G. B. Toward a metabolic theory of ecology. *Ecology* **85**, 1771-1789 (2004).
13 Burton, T., Killen, S. S., Armstrong, J. D. & Metcalfe, N. B. What causes intraspecific variation in resting metabolic rate and what are its ecological consequences? *Proc. R. Soc. Lond. B Biol. Sci.* **278**, 3465-3473, doi:10.1098/rspb.2011.1778 (2011).
14 Biro, P. A. & Stamps, J. A. Do consistent individual differences in metabolic rate promote consistent individual differences in behavior? *Trends Ecol. Evol.* **25**, 653-659, doi:DOI: 10.1016/j.tree.2010.08.003 (2010).
15 Pettersen, A. K., White, C. R. & Marshall, D. J. Metabolic rate covaries with fitness and the pace of the life history in the field. *Proc. R. Soc. Lond. B Biol. Sci.* **283**, 20160323 (2016).
16 McNab, B. K. Ecological factors affect the level and scaling of avian BMR. *Comp. Biochem. Physiol. A* **152**, 22-45 (2009).
17 McNab, B. K. An analysis of the factors that influence the level and scaling of mammalian BMR. *Comp. Biochem. Physiol. A* **151**, 5-28 (2008).
18 Kolokotrones, T., Savage, V. M., Deeds, E. J. & Fontana, W. Curvature in metabolic scaling. *Nature* **464**, 753-756 (2010).
19 White, C. R., Phillips, N. F. & Seymour, R. S. The scaling and temperature dependence of vertebrate metabolism. *Biology Letters* **2**, 125-127 (2006).
20 Speakman, J. R. & Król, E. Maximal heat dissipation capacity and hyperthermia risk: neglected key factors in the ecology of endotherms. *J. Anim. Ecol.* **79**, 726-746 (2010).
21 Speakman, J. R., McDevitt, R. M. & Cole, K. R. Measurement of basal metabolic rates: Don't loose sight of reality in the quest for comparability. *Physiol. Zool.* **66**, 1045-1049 (1993).
22 Hirst, A. G., Glazier, D. S. & Atkinson, D. Body shape shifting during growth permits tests that distinguish between competing geometric theories of metabolic scaling. *Ecol. Lett.* **17**, 1274-1281, doi:10.1111/ele.12334 (2014).
23 Kooijman, S. A. L. M. *Dynamic Energy Budget Theory for Metabolic Organisation*. 3rd edn, (Cambridge University Press, 2010).
24 Killen, S. S., Atkinson, D. & Glazier, D. S. The intraspecific scaling of metabolic rate with body mass in fishes depends on lifestyle and temperature. *Ecol. Lett.* **13**, 184-193 (2010).
25 Witting, L. The body mass allometries as evolutionarily determined by the foraging of mobile organisms. *J. Theor. Biol.* **177**, 129-137, doi:10.1006/jtbi.1995.0231 (1995).
26 Glazier, D. S. *et al.* Ecological effects on metabolic scaling: amphipod responses to fish predators in freshwater springs. *Ecol. Monogr.* **81**, 599-618, doi:10.1890/11-0264.1 (2011).
27 Glazier, D. S. Beyond the '3/4-power law': variation in the intra- and interspecific scaling of metabolic rate in animals. *Biological Reviews* **80**, 622-662 (2005).
28 Glazier, D. S. Is metabolic rate a universal 'pacemaker' for biological processes? *Biological Reviews*, n/a-n/a, doi:10.1111/brv.12115 (2014).
29 Kozłowski, J. & Weiner, J. Interspecific allometries are by-products of body size optimization. *Am. Nat.* **149**, 352-380 (1997).
30 Lande, R. Quantitative genetic analysis of multivariate evolution, applied to brain: body size allometry. *Evolution* **33**, 402-416 (1979).
31 Walsh, B. & Blows, M. W. Abundant genetic variation + strong selection = Multivariate genetic constraints: A geometric view of adaptation. *Annual Review of Ecology,*

Evolution, and Systematics **40**, 41-59, doi:10.1146/annurev.ecolsys.110308.120232 (2009).
32 Zeng, Z.-B. Long-term correlated response, interpopulation covariation, and interspecific allometry. *Evolution* **42**, 363-374, doi:10.2307/2409239 (1988).
33 Tieleman, B. I., Versteegh, M. A., Helm, B. & Dingemanse, N. J. Quantitative genetics parameters show partial independent evolutionary potential for body mass and metabolism in stonechats from different populations. *Journal of Zoology* **278**, 129-136 (2009).
34 Nilsson, J.-Å., Åkesson, M. & Nilsson, J. F. Heritability of resting metabolic rate in a wild population of blue tits. *J. Evol. Biol.* **22**, 1867-1874 (2009).
35 Ronning, B., Jensen, H., Moe, B. & Bech, C. Basal metabolic rate: heritability and genetic correlations with morphological traits in the zebra finch. *J. Evol. Biol.* **20**, 1815-1822, doi:10.1111/j.1420-9101.2007.01384.x (2007).
36 Careau, V. *et al.* Genetic correlation between resting metabolic rate and exploratory behaviour in deer mice (*Peromyscus maniculatus*). *J. Evol. Biol.* **24**, 2153-2163 (2011).
37 Schimpf, N. G., Matthews, P. G. D. & White, C. R. Discontinuous gas exchange exhibition is a heritable trait in speckled cockroaches *Nauphoeta cinerea J. Evol. Biol.* **26**, 1588-1597 (2013).
38 Alton, L. A., Condon, C., White, C. R. & Angilletta, M. J., Jr. Colder environments did not select for a faster metabolism during experimental evolution of *Drosophila melanogaster*. *Evolution* **71**, 145-152, doi:10.1111/evo.13094 (2017).
39 Nespolo, R. F. & Roff, D. A. Testing the aerobic model for the evolution of endothermy: implications of using present correlations to infer past evolution. *Am. Nat.* **183**, 74-83, doi:10.1086/674093 (2014).
40 Delph, L. F., Steven, J. C., Anderson, I. A., Herlihy, C. R. & Brodie III, E. D. Elimination of a genetic correlation bewteen the sexes via artificial correlational selection. *Evolution* **65**, 2872-2880, doi:10.1111/j.1558-5646.2011.01350.x (2011).
41 Roff, D. A. & Fairbairn, D. J. A test of the hypothesis that correlational selection generates genetic correlations. *Evolution* **66**, 2953-2960, doi:10.1111/j.1558-5646.2012.01656.x (2012).
42 Roff, D. A. & Fairbairn, D. J. The evolution of trade-offs under directional and correlational selection. *Evolution* **66**, 2461-2474, doi:10.1111/j.1558-5646.2012.01634.x (2012).
43 Sgrò, C. M. & Hoffmann, A. A. Genetic correlations, tradeoffs and environmental variation. *Heredity* **93**, 241-248, doi:10.1038/sj.hdy.6800532 (2004).
44 Glazier, D. S. The 3/4-power law is not universal: evolution of isometric, ontogenetic metabolic scaling in pelagic animals. *Bioscience* **56**, 325-332 (2006).
45 Kooijman, S. A. L. M. Energy budgets can explain body size relations. *J. Theor. Biol.* **121**, 269-282, doi:Doi: 10.1016/s0022-5193(86)80107-2 (1986).
46 Maino, J. L., Kearney, M. R., Nisbet, R. M. & Kooijman, S. A. L. M. Reconciling theories for metabolic scaling. *J. Anim. Ecol.*, DOI: 10.1111/1365-2656.12085, doi:10.1111/1365-2656.12085 (2013).
47 Lighton, J. R. B. *Measuring metabolic rates: a manual for scientists*. (Oxford University Press, 2008).
48 Wilson, A. J. Why h^2 does not always equal V_A/V_P? *J. Evol. Biol.* **21**, 647-650 (2008).
49 Gilmour, A. R., Gogel, B. J., Cullis, B. R. & Thompson, R. *ASReml user guide. Release 3.0*. (NSW Department of Industry and Investment, 2009).
50 White, I. R pin function. http://www.homepages.ed.ac.uk/iwhite//asreml/. (2013).
51 Revell, L. J. phytools: an R package for phylogenetic comparative biology (and other things). *Methods in Ecology and Evolution* **3**, 217-223 (2012).

52 R: A Language and Environment for Statistical Computing. v. 3.2.2 (R Foundation for Statistical Computing, Vienna, Austria, 2016).
53 Bininda-Emonds, O. R. P. *et al.* The delayed rise of present-day mammals. *Nature* **446**, 507-512 (2007).
54 Jones, K. E. *et al.* PanTHERIA: a species-level database of life history, ecology, and geography of extant and recently extinct mammals. *Ecology* **90**, 2648 (2009).
55 Frappell, P. B. & Butler, P. J. Minimal metabolic rate, what it is, its usefulness, and its relationship to the evolution of endothermy: a brief synopsis. *Physiol. Biochem. Zool.* **77**, 865-868 (2004).
56 Butler, P. J., Green, J. A., Boyd, I. L. & Speakman, J. R. Measuring metabolic rate in the field: the pros and cons of the doubly labelled water and heart rate methods. *Funct. Ecol.* **18**, 168-183 (2004).
57 Dlugosz, E. M. *et al.* Phylogenetic analysis of mammalian maximal oxygen consumption during exercise. *J. Exp. Biol.* **216**, 4712-4721 (2013).
58 Norin, T. & Clark, T. D. Measurement and relevance of maximum metabolic rate in fishes. *J. Fish Biol.* **88**, 122-151, doi:10.1111/jfb.12796 (2016).
59 Lynch, M. Methods for the analysis of comparative data in evolutionary biology. *Evolution* **45**, 1065-1080, doi:10.2307/2409716 (1991).
60 Housworth, E. A., Martins, E. P. & Lynch, M. The phylogenetic mixed model. *Am. Nat.* **163**, 84-96, doi:10.1086/380570 (2004).
61 Hadfield, J. D. & Nakagawa, S. General quantitative genetic methods for comparative biology: phylogenies, taxonomies and multi-trait models for continuous and categorical characters. *J. Evol. Biol.* **23**, 494-508 (2010).
62 Hinchliff, C. E. *et al.* Synthesis of phylogeny and taxonomy into a comprehensive tree of life. *Proceedings of the National Academy of Sciences* **112**, 12764-12769, doi:10.1073/pnas.1423041112 (2015).
63 Hadfield, J. D. MCMC methods for multi-response generalized linear models: the MCMCglmm R Package. *Journal of Statistical Software* **33** (2010).
64 Schluter, D. Adaptive radiation along genetic lines of least resistance. *Evolution* **50**, 1766-1774 (1996).

Fig. 1. Phylogenetic distribution of the genetic correlation (r_G) between metabolic rate and body mass. Species are (from top to bottom): African stonechat *Saxicola torquata*[33] (estimate for *Saxicola torquata axillaris* plotted above that for *Saxicola torquata rubicola*), blue tit *Cyanistes caeruleus*[34], zebra finch *Taeniopygia guttata*[35], deer mouse *Peromyscus maniculatus*[36], *Drosophila melanogaster*, *Drosophila serrata*, Cockroach *Nauphoeta cinerea* (the estimate for females is plotted above that for males). Dotted lines correspond with values of r_G of -1 and +1; the dashed line corresponds with r_G = 0. Data are shown ± SE, the tree was dated using www.timetree.org, endothermic species are coloured red, ectothermic species are coloured blue.

Fig. 2. Relationship between metabolic rate and body mass predicted by random evolution. Results are for 4000 tips evolving on a random tree, with a genetic correlation between metabolic rate and body mass (r_G = 0.78, Fig. 1), a variance of 0.025 for log-transformed body mass and a variance of 0.0183 for log-transformed metabolic rate, calculated from the mean ratio of σ^2_{MR} to σ^2_M; 0.73, see text for details). Orange lines are density contours corresponding to (from inner to outer contour) the 50th, 80th, 90th, and 95th percentiles. Dashed lines represent (from top to bottom) scaling exponents of 1, 0.75, and 0.5.

Fig. 3. Empirical and simulated distributions of metabolic scaling exponents and mass-independent variation in metabolic rate. (a) Empirical scaling exponent of metabolic rate for a range of species measured at rest (circles), while free living (squares), or during intense activity (diamonds) shown ± 95% CI. Groups that are predominantly endothermic are coloured red, groups that are predominantly ectothermic are coloured blue. (b) Grey bars depict the distribution of simulated scaling exponents under a model of random evolution with a genetic correlation. The vertical dashed line represents the scaling exponent of ¾ predicted by several metabolic theories[4,5,45,46]. (c) Standard deviation of the variation in metabolic rate that is not explained by variation in body mass or temperature (residual variation) for the relationships in (a). (d) Standard deviation of the variation in metabolic rate that is not explained by variation in body mass for the relationships in (b).

Fig. 4. Metabolic scaling relationships are not consistent with random evolution under a genetic constraint alone. In the upper panel, the black dots depict the combinations of scaling exponents and residual standard deviation that are produced by 100,000 simulations of the evolution of metabolic rate and body mass by random evolution under a genetic constraint with genetic correlations modelled based on their empirical distribution (see text for details). Orange lines are (inner to outer) 50th, 70th, 90th and 95th percentile density contours of the 100,000 simulated exponents. Red and blue symbols represent empirical metabolic scaling exponents for endotherms and ectotherms, respectively, for animals measured at rest (circles), while free living (squares), or during intense activity (diamonds) shown ± 95% CI. The area enclosed by the dashed box in the upper panel is reproduced in the lower panel for clarity.

Fig. 5. The phylogenetic diversity of metabolic rate and body mass. (A) Ellipse outlining the additive genetic ("breeding") values of individuals within a population. The shading in panel a) depicts the fitness surface (darker shading corresponds with higher fitness) describing the pattern of correlational selection on metabolic rate and body mass hypothesized to generate the additive genetic correlation between metabolic rate and mass, and to constrain the evolution of mass-independent metabolic rate. The long axis of the ellipse is the direction of greatest genetic variance, $\mathbf{g}_{max}$, which represents the genetic line of least resistance[64] depicted by the dashed line. If the additive genetic variance-covariance matrix is stable through time, evolution should proceed along the direction of $\mathbf{g}_{max}$ in the absence of selection, yielding strongly correlated phenotypic values of metabolic rate and body mass, as is observed for extant species (the lengths of the light grey bars in panel b are proportional to $\log_{10}$-transformed body mass; dark grey bars are proportional in length to $\log_{10}$-transformed resting metabolic rate). The observed additive genetic correlation between metabolic rate and body mass for a range of animals (Fig. 1) predicts the among-species relationship between metabolic rate and body mass (the slopes of the solid lines for the scaling of resting metabolic rates in panels c-h) are the median simulated values for endotherms and ectotherms from Fig. 3b; colours correspond with clades in panel b).

461
462
463

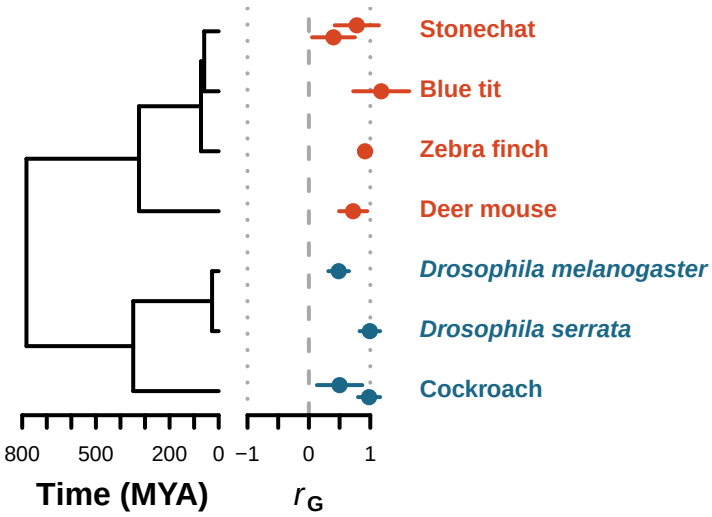
Stonechat
Blue tit
Zebra finch
Deer mouse
Drosophila melanogaster
Drosophila serrata
Cockroach
800
500
200
0
−1
0
1
Time (MYA)
r_G

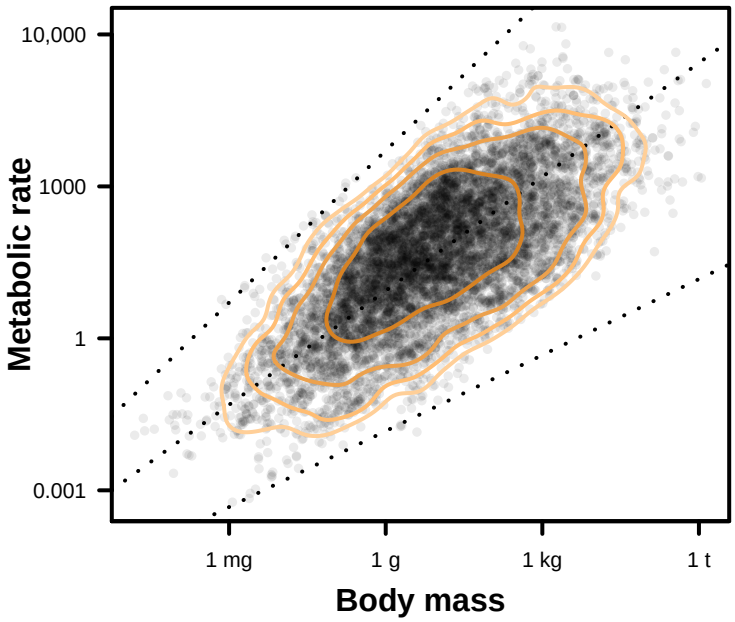
10,000
1000
1
0.001
Metabolic rate
1 mg
1 g
1 kg
1 t
Body mass

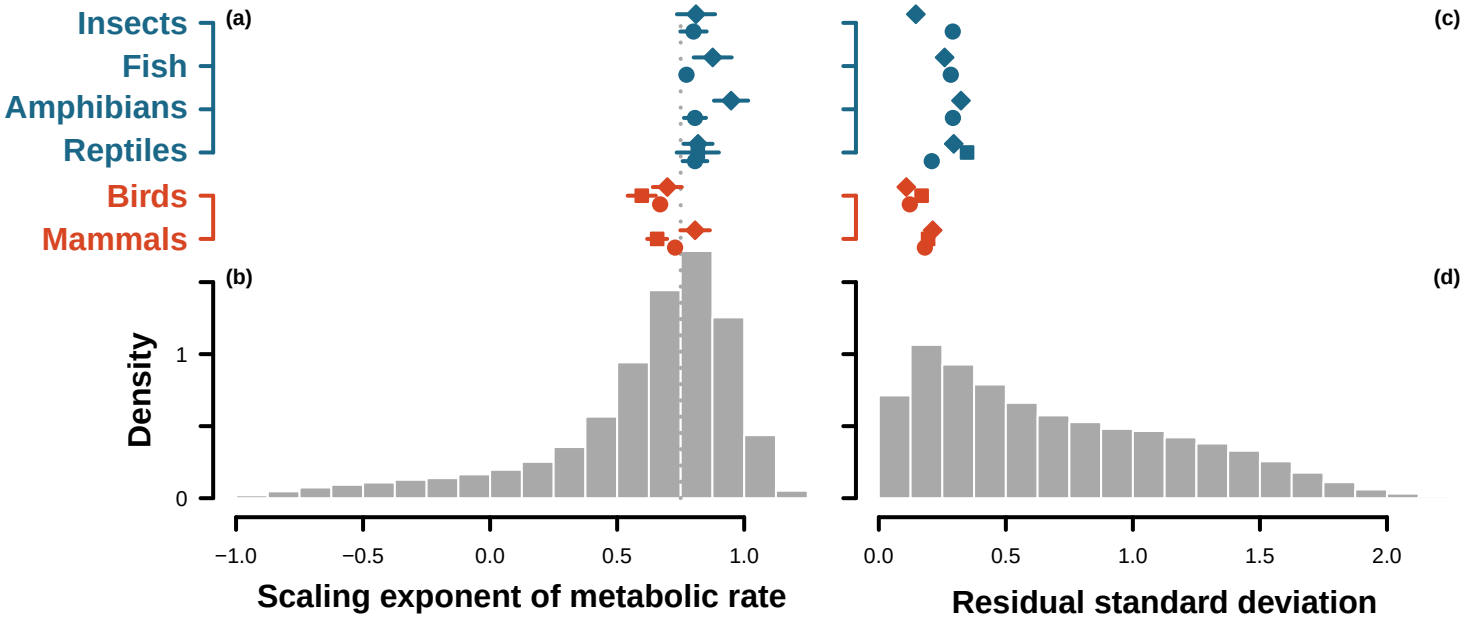
Insects
Fish
Amphibians
Reptiles
Birds
Mammals
(a)
(b)
(c)
(d)
Density
0
1
−1.0
−0.5
0.0
0.5
1.0
Scaling exponent of metabolic rate
0.0
0.5
1.0
1.5
2.0
Residual standard deviation

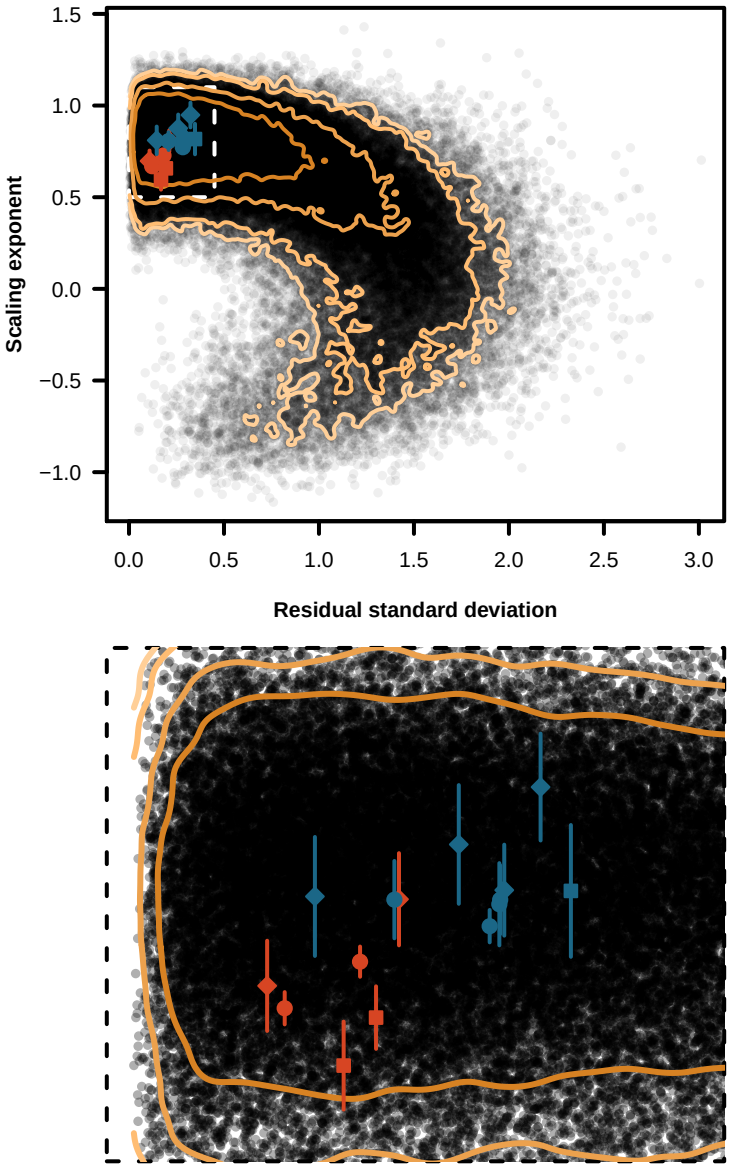
1.5
1.0
0.5
0.0
−0.5
−1.0
Scaling exponent
0.0
0.5
1.0
1.5
2.0
2.5
3.0
Residual standard deviation

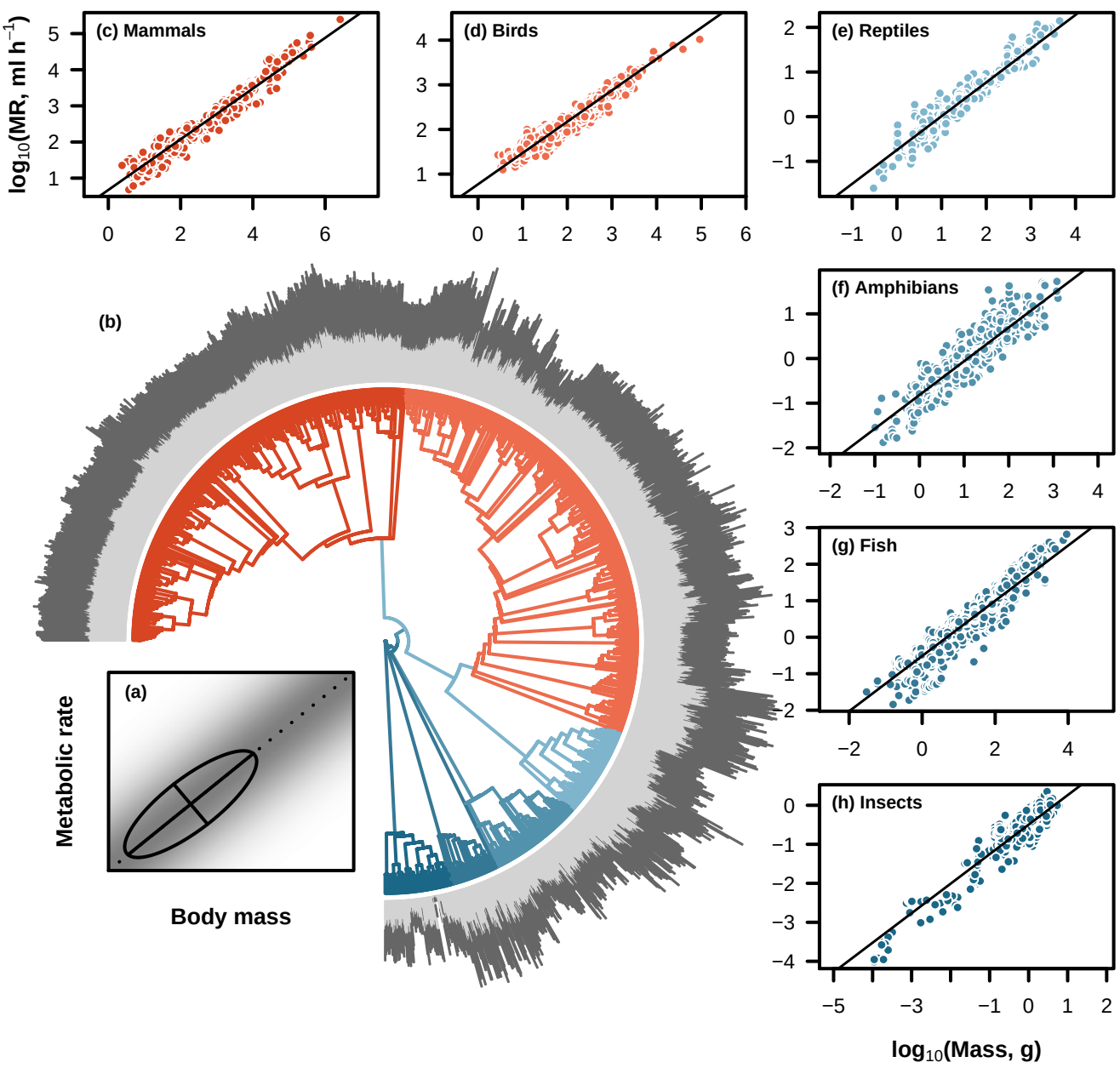
(a)
Metabolic rate
Body mass
(b)
(c) Mammals
(d) Birds
(e) Reptiles
(f) Amphibians
(g) Fish
(h) Insects
log10(MR, ml h−1)
log10(Mass, g)